Huchon, P., Taylor, B., and Klaus, A. (Eds.)
Proceedings of the Ocean Drilling Program, Scientific Results Volume 180

21. Data Report: Magnetic Anisotropy of Samples in a Fault Zone at ODP Site 1117 in the Western Woodlark Basin (Papua New Guinea)[1]

Naoto Ishikawa[2] and Gina Marie Frost[3]

ABSTRACT

At Site 1117, drilled during Leg 180 of the Ocean Drilling Program in the Woodlark Basin, we cored a fault zone and recovered fault gouge, mylonitized and brecciated gabbros, and undeformed gabbro. We measured the anisotropy of magnetic susceptibility for the rock samples. The susceptibilities of the fault gouge samples were lower than those of the undeformed gabbro, and those of deformed gabbros were lowest. The anisotropy degrees of the fault gouge samples were higher than those of the deformed and undeformed gabbros. Oblate magnetic fabrics were dominant in the samples from the fault zone.

INTRODUCTION

One of the primary objectives of Ocean Drilling Program Leg 180 was to characterize the composition and in situ properties of an active low-angle normal fault zone to understand how such faults slip. Site 1117 is on the upper slope of the northern flank of Moresby Seamount where the fault surface of a low-angle normal fault cropped out. Rotary core barrel (RCB) coring was used at three holes. RCB cores indicated that the minimum thickness of a shear zone was ~100 m on the footwall (Shipboard Scientific Party, 1999). We measured the magnetic anisotropy and rock magnetic properties on samples collected from the shear zone. Magnetic fabrics and rock magnetic parameters have been shown

[1]Ishikawa, N., and Frost, G.M., 2001. Data report: Magnetic anisotropy of samples in a fault zone at ODP Site 1117 in the western Woodlark Basin (Papua New Guinea). *In* Huchon, P., Taylor, B., and Klaus, A. (Eds.), *Proc. ODP, Sci. Results,* 180, 1–7 [Online]. Available from World Wide Web: <http://www-odp. tamu.edu/publications/180_SR/VOLUME/CHAPTERS/174.PDF>. [Cited YYYY-MM-DD]
[2]Graduate School of Human and Environmental Studies, Kyoto University, Sakyo-ku, Kyoto 606-8501, Japan.
ishikawa@gaia.h.kyoto-u.ac.jp
[3]Central Oregon Community College, 2600 Northwest College Way, Bend OR 97701-5998, USA.

Initial receipt: 14 December 2000
Acceptance: 12 July 2001
Web publication: 20 November 2001
Ms 180SR-174

to provide useful information that reveal deformation features in fault zones (e.g., MacDonald and Ellwood, 1987; Tarling and Hrouda, 1993). In this chapter, we report data on the anisotropy of magnetic susceptibility (AMS) obtained from the samples described above.

SAMPLES AND METHOD

Among the three holes at Site 1117, Hole 1117A (9°46.526′S, 151°32.945′E) was cored to 111.1 meters below seafloor. Noncumulate quartz magnetite gabbros were recovered at the base. Brecciated and then mylonitized equivalents in the cores above the base showed an upward-increasing shearing and alteration, and in the surficial core ~4 m of fault gouge was recovered. Shipboard analysis defined the following four structural domains (Shipboard Scientific Party, 1999):

Domain I, fault gouge, in Cores 180-1117A-1R and 2R;
Domain II, mylonite zone, in Cores 180-1117A-2R to 7R;
Domain III, brecciated zone, in Cores 180-1117A-8R to 12R; and
Domain IV, undeformed zone, in Cores 180-1117A-13R and 14R.

Soft clayey material comprised the fault gouge of Domain I and consisted of a mixture of talc, chlorite, ankerite, and serpentine. These minerals were alteration products of the gabbro found at the base. The initial structure in the fault gouge was difficult to assess because of coring-related deformation. In Domain II, epidote-rich metamorphic rocks recovered were mylonites and cataclastites showing developed anastomosing foliation planes, shear bands, and fibrous quartz pressure shadows. Major minerals were epidote, quartz, chlorite, and calcite. Domain III was defined by the brecciation of gabbroic rocks. Metamorphism by hydrothermal alteration was inferred in the rocks. Domain IV consisted of an undeformed magnetite-quartz gabbro with noncumulate structure. Undeformed fresh gabbros were also recovered in Core 180-1117A-11R in Domain III.

We collected 13 cubic samples from Domain I using 8-cm³ plastic cubes (2 cm × 2 cm × 2 cm). Five cubic samples were also cut out from rock pieces of deformed gabbros in Domains II and III (four) and an undeformed gabbro in Domain III (Sample 180-1117A-11R [Piece 7]). Among the 15 samples, the AMS of six samples was measured on board ship with a KLY-2 susceptibility meter (AGICO, Inc.); the remaining samples were measured after Leg 180 using a KLY-3S susceptibility meter (AGICO, Inc.) at Kyoto University. The corrected anisotropy degree (P_j) and shape parameter (T) of the susceptibility ellipsoid were calculated after Jelinek (1981). The AMS parameters obtained are reported in this chapter, including results from onboard measurements.

RESULTS AND DISCUSSION

AMS results are listed in Table T1 and plotted in Figures F1 and F2. Initial mean volume susceptibilities of samples showed a distinctive feature. Fault gouge samples of Domain I had susceptibilities of 10^{-3} to 10^{-2} SI. An undeformed gabbro sample, the protolith of the gouge, showed the highest value, whereas susceptibilities of deformed gabbro samples from Domains II and III were $<10^{-3}$ SI. The susceptibility values imply that the main carrier of AMS is a ferrimagnetic mineral for the gouge

T1. Results of AMS measurements, p. 7.

F1. Plots of AMS parameters, p. 5.

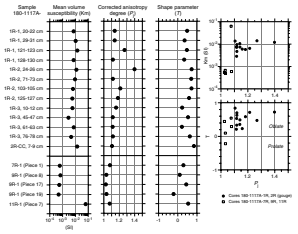

F2. Orientations of principal susceptibility axes of magnetic fabrics, p. 6.

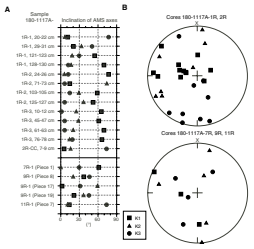

and undeformed gabbro samples, whereas the contribution of both ferrimagnetic and paramagnetic minerals to the AMS may be inferred for the deformed gabbros (Tarling and Hrouda, 1993). The acquisition curves of isothermal remanent magnetization showed that the gouge and deformed/undeformed gabbro samples were saturated at ~0.2 T (Shipboard Scientific Party, 1999), which implies the presence of magnetite and/or maghemite. Petrological observations on board ship indicated the existence of magnetite in undeformed gabbro (Shipboard Scientific Party, 1999). Magnetite may be considered a principal AMS carrier in the undeformed gabbro. The gouge samples in Domain I consisted of hydrothermal alteration products and deformed gabbros in Domain II and III that were subjected to hydrothermal alteration (Shipboard Scientific Party, 1999). The existence of maghemite might have been inferred in the gouge and deformed gabbro samples as one of ferrimagnetic minerals that contribute to the AMS. Further rock magnetic analysis will be needed to identify AMS carriers.

The P_j values of the fault gouge samples were >1.1, and those of the deformed and undeformed gabbros were <1.1 (Fig. F1). All samples but one showed positive T values, that is, the fabrics had an oblate shape. The oblateness of the magnetic fabric appeared to increase as the P_j value increased. Shallow inclinations of K3 axes (<30°) were dominant, indicating that magnetic foliation planes were close to vertical (Fig. F2). Because drilling-related deformation was observed in the fault gouge cores (Shipboard Scientific Party, 1999), these AMS features might be attributed to a coring effect.

Gabbro samples showed low P_j values (<1.1), especially the brecciated gabbros of Domain III (Core 180-1117A-9R) had the lowest values (Fig. F1). The T values for the deformed gabbros ranged between –0.22 and 0.44 and were lower than those for the undeformed gabbro (Sample 180-1117A-11R-1, piece 7). K3 axes of the deformed gabbros had moderate inclinations, whereas the undeformed gabbro sample yielded a subhorizontal magnetic foliation with steep inclination of the K3 axis (Fig. F2). Structural analysis on the deformed and undeformed gabbro samples will be necessary to clarify the relationship between the magnetic fabrics and deformation features of the rocks.

ACKNOWLEDGMENTS

This research used samples and/or data provided by the Ocean Drilling Program (ODP). ODP is sponsored by the U.S. National Science Foundation (NSF) and participating countries under management of Joint Oceanographic Institutions (JOI), Inc.

We thank all participants of the Leg 180 shipboard scientific party, the technicians, and the crew of the *JOIDES Resolution*. We also thank Drs. B. Taylar and E. Herrero-Bervera for their kind reviews.

REFERENCES

Jelinek, V., 1981. Characterization of the magnetic fabric of rocks. *Tectonophysics,* 79:63–67.

MacDonald, W.D. and Ellwood, B.B., 1987. Anisotropy of magnetic susceptibility: sedimentological, igneous, and structural-tectonic applications, *Rev. Geophys*., 25: 905–909.

Shipboard Scientific Party, 1999. Site 1117. *In* Taylor, B., Huchon, P., Klaus, A., et al., *Proc. ODP, Init. Repts.,* 180, 1–45 [CD-ROM]. Available from: Ocean Drilling Program, Texas A&M University, College Station, TX 77845-9547, U.S.A.

Tarling, D.H., and Hrouda, F., 1993. *The Magnetic Anisotropy of Rocks:* London (Chapman and Hall).

Figure F1. Plots of AMS parameters.

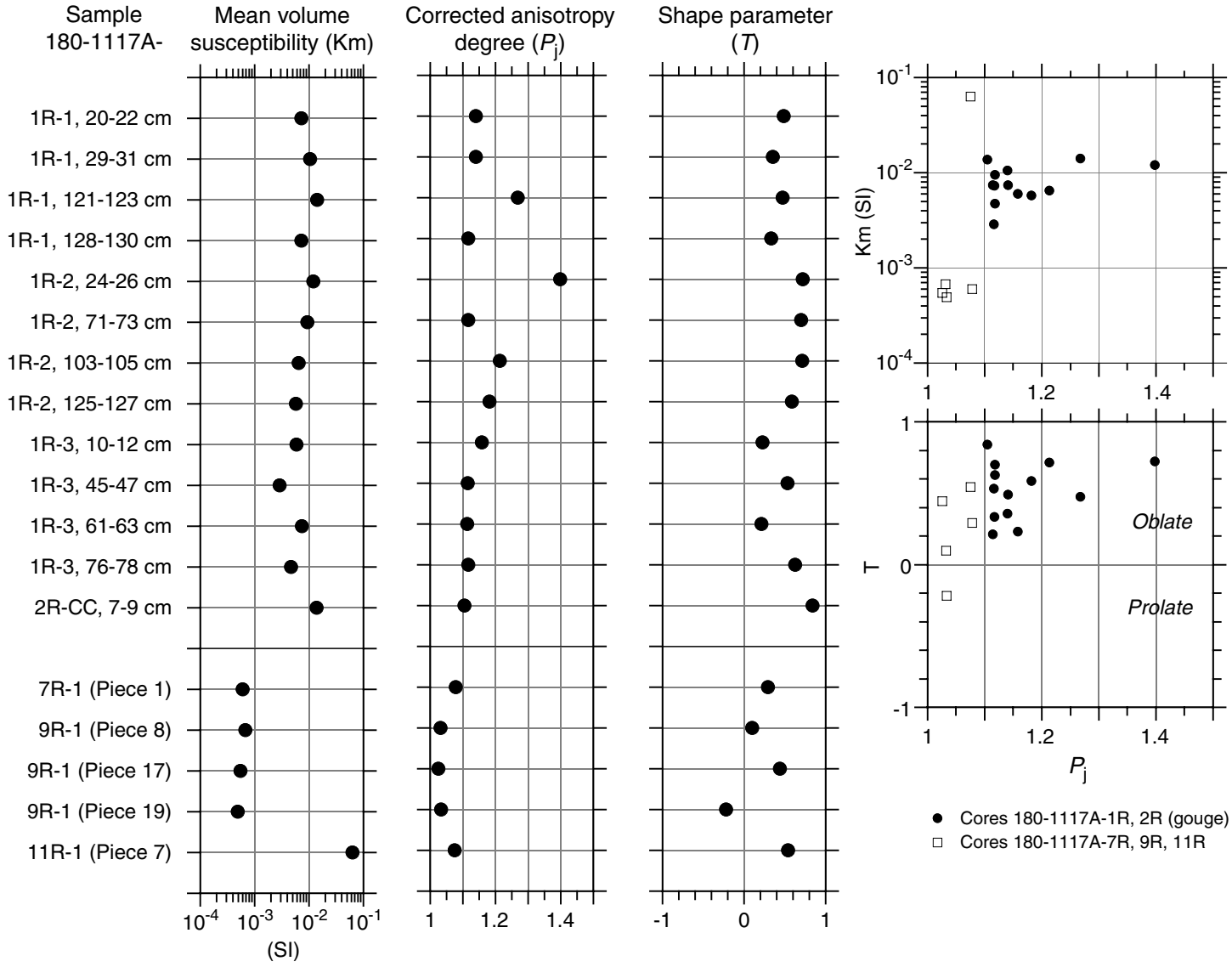

Figure F2. Orientations of the principal susceptibility axes of magnetic fabrics. **A.** Inclination values of the principal axes. **B.** Equal-area projection of the axes. The directions of the maximum (K1), intermediate (K2), and minimum (K3) principal axes are plotted as squares, triangles and circles, respectively. Solid symbols are on the lower hemisphere.

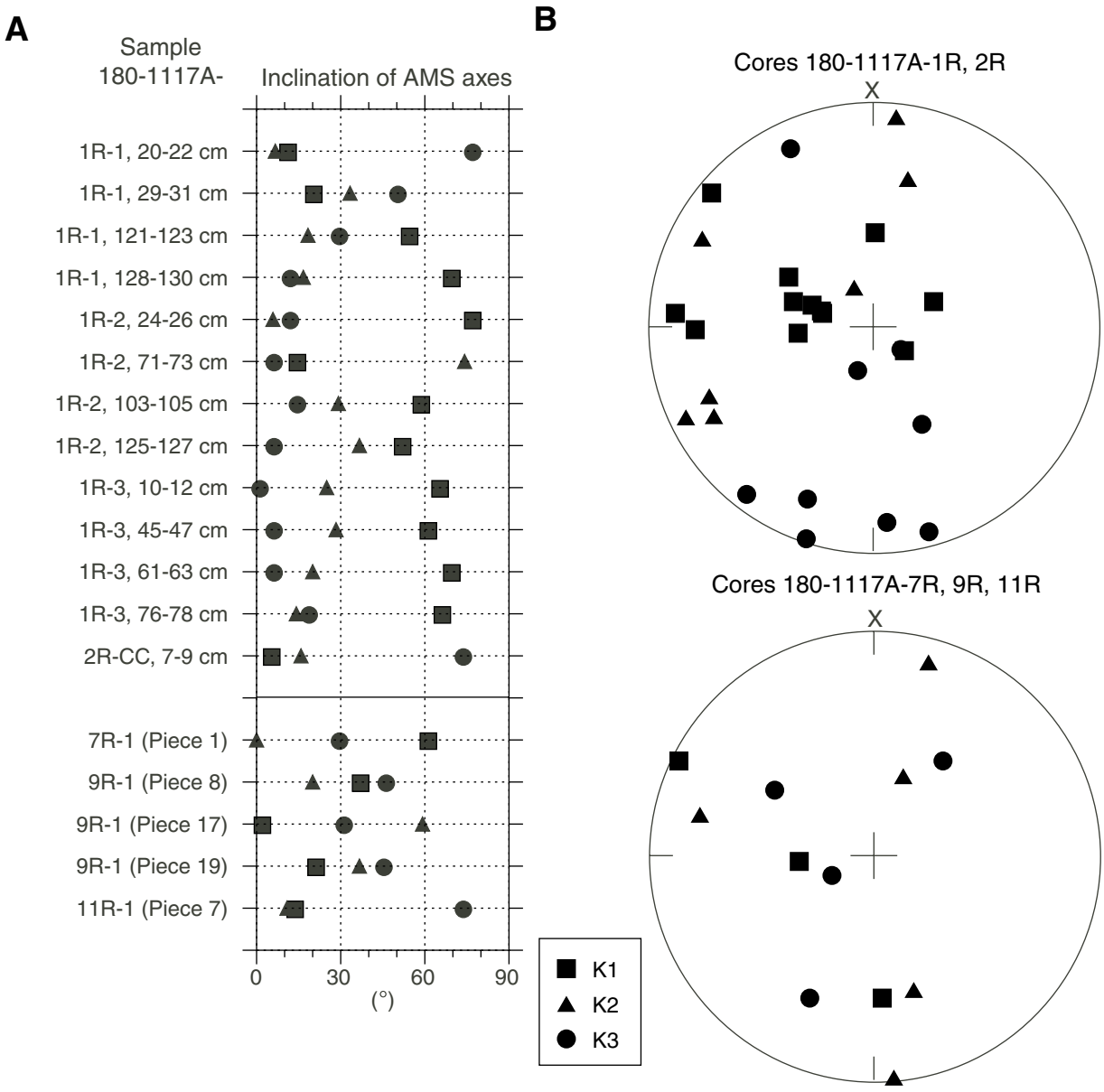

Table T1. Results of AMS measurements, Site 1117.

Core, section, interval (cm)	Volume (cm^3)	Mean volume susceptibility, Km (SI)	Normalized susceptibility of principal axes			Degree of anisotropy (P_j)	Shape parameter (T)	Direction of principal axes (°)					
								K1		K2		K3	
			K1 maximum	K2 intermediate	K3 minimum			Declination	Inclination	Declination	Inclination	Declination	Inclination
180-1117A-													
1R-1, 20–22*	8.00	7.373E–3	1.0529	1.0194	0.9277	1.141	0.489	275	11	6	7	130	77
1R-1, 29–31	8.00	1.058E–2	1.0567	1.0139	0.9294	1.140	0.356	270	20	13	33	154	50
1R-1, 121–123	8.00	1.409E–2	1.0961	1.0322	0.8717	1.268	0.476	359	54	541	18	140	29
1R-1, 128–130	8.00	7.309E–3	1.0485	1.0112	0.9403	1.117	0.335	290	69	148	17	54	12
1R-2, 24–26	8.00	1.204E–2	1.1144	1.0674	0.8182	1.398	0.721	127	77	244	6	335	12
1R-2, 71–73	8.00	9.452E–3	1.0394	1.0234	0.9372	1.118	0.700	127	14	329	74	218	6
1R-2, 103–105	8.00	6.484E–3	1.0672	1.0402	0.8926	1.213	0.713	289	58	78	29	176	14
1R-2, 125–127*	8.00	5.770E–3	1.0636	1.0290	0.9074	1.182	0.584	301	52	138	37	42	8
1R-3, 10–22*	8.00	5.983E–3	1.0676	1.0094	0.9230	1.158	0.230	290	65	108	25	198	1
1R-3, 45–47	8.00	2.881E–3	1.0430	1.0177	0.9393	1.116	0.531	266	61	71	28	165	6
1R-3, 61–63	8.00	7.449E–3	1.0500	1.0066	0.9434	1.114	0.211	288	69	127	20	34	6
1R-3, 76–78	8.00	4.711E–3	1.0413	1.0211	0.9376	1.118	0.627	63	66	297	14	202	18
2R-CC, 7–9*	8.00	1.378E–2	1.0320	1.0246	0.9435	1.105	0.839	310	5	41	16	203	73
7R-1 (Piece 1)	7.89	6.009E–4	1.0335	1.0068	0.9597	1.078	0.293	266	61	275	0	85	29
9R-1 (Piece 8)	8.42	6.744E–4	1.0153	1.0010	0.9838	1.032	0.100	177	37	284	20	36	46
9R-1 (Piece 17)*	10.77	5.460E–4	1.0105	1.0036	0.9859	1.026	0.444	296	2	20	59	205	31
9R-2 (Piece 19)	8.95	4.895E–4	1.0172	0.9976	0.9852	1.033	-0.217	56	21	163	37	304	45
11R-1 (Piece 7)*	6.78	6.333E–2	1.0282	1.0121	0.9597	1.075	0.542	109	13	16	11	246	73

Note: * = measured on board.